10 h 18

| This work presents the first time-domain analysis of pulse propagation through stable, balanced nonlinear periodic structures, with a focus on design towards all-optical signal processing applications. The propagation dynamics of ultrashort pulses in the nonlinear structures with | Đây là công trình đầu tiên phân tích quá trình lan truyền xung qua cấu trúc tuần hoàn phi tuyến ổn định, cân bằng trong miền thời gian, ở đây chúng ta sẽ tập trung vào thiết kế nhằm phục vụ các ứng dụng xử lý tín hiệu toàn quang. Chúng ta sẽ nghiên cứu đặc tính động học của quá trình lan truyền xung cực |

varying grating lengths and linear grating strengths are investigated. In the absence of a linear grating, with two adjacent layers of nonlinear materials (n1,2 = 1.50 ± (2.5 x 10-12 cm2/GW)/in), the pulse-bandwidth-dependent limiting behavior is investigated. The output peak intensity of a 600 fs input pulse is found to be limited to 1.2 GW/cm2 for a 290 ^m-long device. In the presence of a linear grating, S- and N-curve transfer characteristics are observed. A 720 ^m-long device with a 0.01 out-of¬phase linear grating (i.e., n1,2 = (1.50 ^ 0.01) ± (2.5 x 10-12 cm2/GW)/in), compresses a pulse down to 12% of its original width. The results reported in this work point to the promise of such devices in signal processing.

Motivation

Telecommunications networks now play an extremely important role in a world where global communication has become an essential element of everyday life. These networks demand great bandwidth for networking applications such as data browsing and massive file transfer on the Internet, multimedia-on-demand, video conferencing, and much more.

To meet the increasing demand, economical and efficient technologies that provide higher capacity and improved networking are critical. Optical networking is the foremost of such technologies because it can offer higher speeds over long transmission distances, providing unbeatable cost-per-bandwidth due to the low loss and managed dispersion of optical fiber over a wide spectrum.

ngắn trong các cấu trúc phi tuyến có chiều dài cách tử biến đổi và mật độ cách tử tuyến tính. Đặc tính giới hạn cường độ theo dải thông xung của hai lớp vật liệu tiếp giáp nhau (n1,2 = 1.50 ± (2.5 x 10-12 cm2/GW)/in) khi không có cách tử tuyến tính được nghiên cứu. Đối với thiết bị dài 290 ^m, cường độ cực đại đầu ra của xung đầu vào 600 fs giới hạn ở mức 1.2 GW/cm2. Khi có cách tử tuyến tính, đường cong đặc tuyến truyền có dạng hình chữ S hoặc N. Thiết bị dài 720 ^m với cách tử tuyến tính lệch pha 0.01 (tức là , n1,2 = (1.50 ^ 0.01) ± (2,5 x 10-12 cm2 / GW) / in) nén xung đến 12% độ rộng ban đầu của nó. Các kết quả được báo cáo trong công trình này hứa hẹn khả năng phát triển những thiết bị ứng dụng trong xử lý tín hiệu.
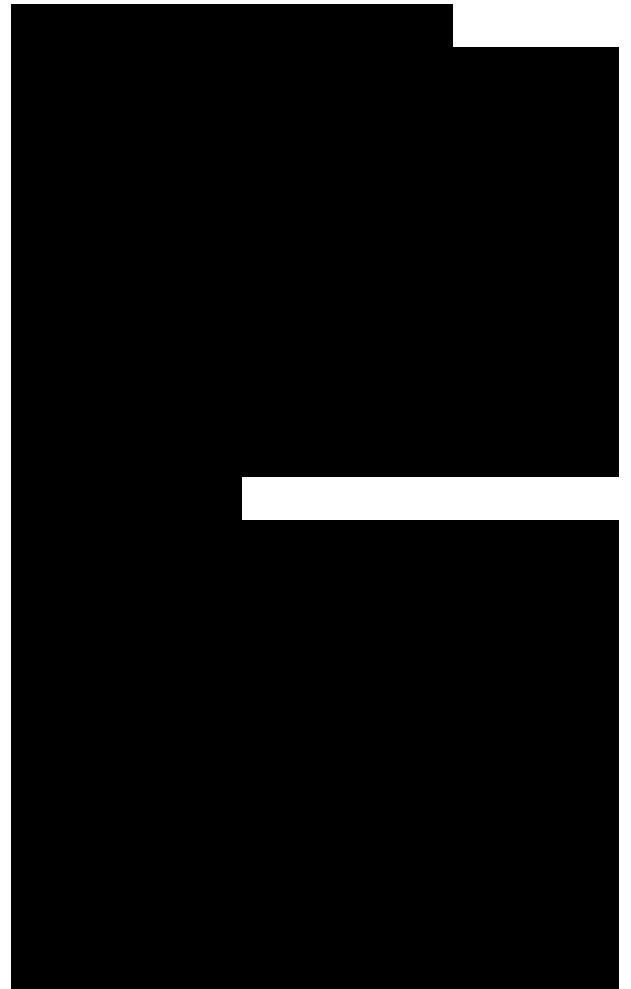
In principle, the maximum information capacity of a standard, commercially available optical fiber over 100 kilometers is around 3 b/s/Hz [1]. Coupled with a maximum fiber bandwidth of ~ 50 THz (corresponding to a wavelength range from 1.2 to 1.6 ^m), this means that an ultimate 150 Tb/s can be achieved. In practice, however, commercial networks are not capable of operating close to this rate. The transmission of multiple signals simultaneously over the same fiber provides a simple way for making use of the abundant information capacity offered by fiber optics [2]. In order to achieve the highest possible transmission rate, signal multipexing techniques - wavelength-division multiplexing (WDM) and time-division multiplexing (TDM) - are commonly employed. In March 2001, NEC Corporation set a new fiber optic transmission record of 10.9 Tb/s by transmitting 273 channels of data at 40 Gb/s per channel over 117 kilometers. However, the bit rate per channel is often limited to 40 Gb/s in commercial systems due to the speed of electronic components, and the optical limitations imposed by fiber dispersion and fiber nonlinearity. The two signal multiplexing techniques, WDM and TDM, are explained further in the next section.

1.2.1 Mach-Zehnder Interferometer

A nonlinear Mach-Zehnder interferometer has a nonlinear element on one of the two parallel arms, as illustrated in Figure 1.1 [4]. In the nonlinear element, the properties of

Figure 1.1: A nonlinear Mach-Zehnder Interferometer (MZ).
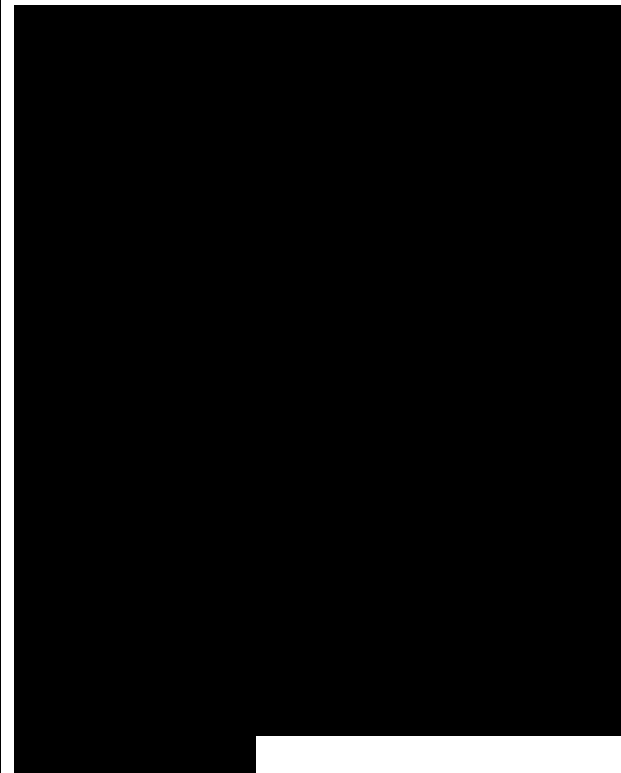
the medium are dependent on the intensity of the supplied optical field. In other words, the presence of an optical field modifies the properties of the medium, which in turn, modifies another optical field or the original field itself. The refractive index (u) of a nonlinear material can be expressed as:

$$u = n_0 + u_2 I, \qquad (1.1)$$

where u_0 is the linear part of the refractive index, and u_2 is the Kerr coefficient of the material. In the case of the Mach-Zehnder interferometer, the control signal modifies the data signal by altering the phase shift experienced by the signal traveling in the nonlinear arm. In the absence of the control signal, the low-power data signal is split into the two arms at the input and is recombined at the output port where the two optical fields interfere constructively. Thus the input pulse is reproduced at the output. If a control signal is present such that a n relative phase shift is introduced between the two arms, the optical fields recombine at the output port and interfere destructively. The result is no output. A Mach-Zehnder interferometer can therefore act to switch signals on and off depending on the the control signal. This is in effect a logic NAND operation. If two control signals are introduced, one for each nonlinear arm, the Mach-Zehnder interferometer can behave as a two-input XOR gate.

1.2.2 Fabry-Perot Resonator

A Fabry-Perot resonator consists of two parallel, highly reflective mirrors separated by a distance d. In a nonlinear Fabry-Perot device, the medium in between the mirrors is optically nonlinear, as shown in Figure 1.2(a).

The input-output relation for this system (Figure 1.2(b)) forms a hysteresis loop, making this device a bistable system. By definition, a bistable system has an output that can take only one of two distinct stable values [4]. Switching between these values may be achieved by a temporary change of the level of the input. At a low input power (point a), the nonlinear effect is negligible,

(b)

Figure 1.2: (a) A nonlinear Fabry-Perot resonator. (b) Input-output relation: a bistable system (reproduced from [5]).

resulting in low transmission. As the input power is increased, the power accumulates in the resonator, but the transmission remains relatively low, until point c (threshold intensity Ith2) is reached. Further increase of the input power switches the device to a high-transmission state (point d) because the device operates near the resonance. At a higher input power (point e), the device is tuned away from the resonance, therefore reducing the power in it. As the input power is decreased, the device will remain in the high-transmission state until point f (threshold intensity Ithi) is reached. For a lower input power, the device will switch to the low-transmission state (point b) because the device is further away from the resonance. This process is described in detail by Smith et al. [5]. The system therefore takes its low value for small inputs (I < Ith1) and its high value for large inputs (I > Ith2), where Ith\ and Ith2 are the thresholds as shown in Figure 1.2(b). In the intermediate range, Ith\ < Iin < Ith2, however, any slight change forces the output to either the upper or lower branch depending on the

initial state. Thus, such a bistable device can function as a switch, a logic gate, and a memory element.

1.2.3 Directional Coupler

When two waveguides are sufficiently close, light can be coupled from one waveguide to the other. A nonlinear direction coupler works based on this principle (Figure 1.3 [4]). The refractive indices and the dimensions of the waveguides may be selected so that when

Figure 1.3: A nonlinear directional coupler (sorting a sequence of weak and strong pulses).

the input optical power is low, it is channeled into the other waveguide; when it is high the refractive indices are altered in the nonlinear material and the power remains in the same waveguide [4]. The detuning induced by the Kerr nonlinearity effectively switches the input signal from one waveguide to the other. Besides switching and performing logic operations, the device can be also used to sort a sequence of weak and strong pulses, separating them into the the two output ports of the coupler, as illustrated in Figure 1.3.

1.2.5 Periodic Structure

A simple nonlinear periodic structure consists of alternating layers of linear and nonlin¬ear materials, as shown in Figure 1.5. As a light beam propagates through a nonlinear

Figure 1.5: Schematic of a simple nonlinear periodic structure with periodicity A. The two adjacent layers consist of one linear material with refractive index na and one non¬linear material with intensity-dependent refractive index nb(I).
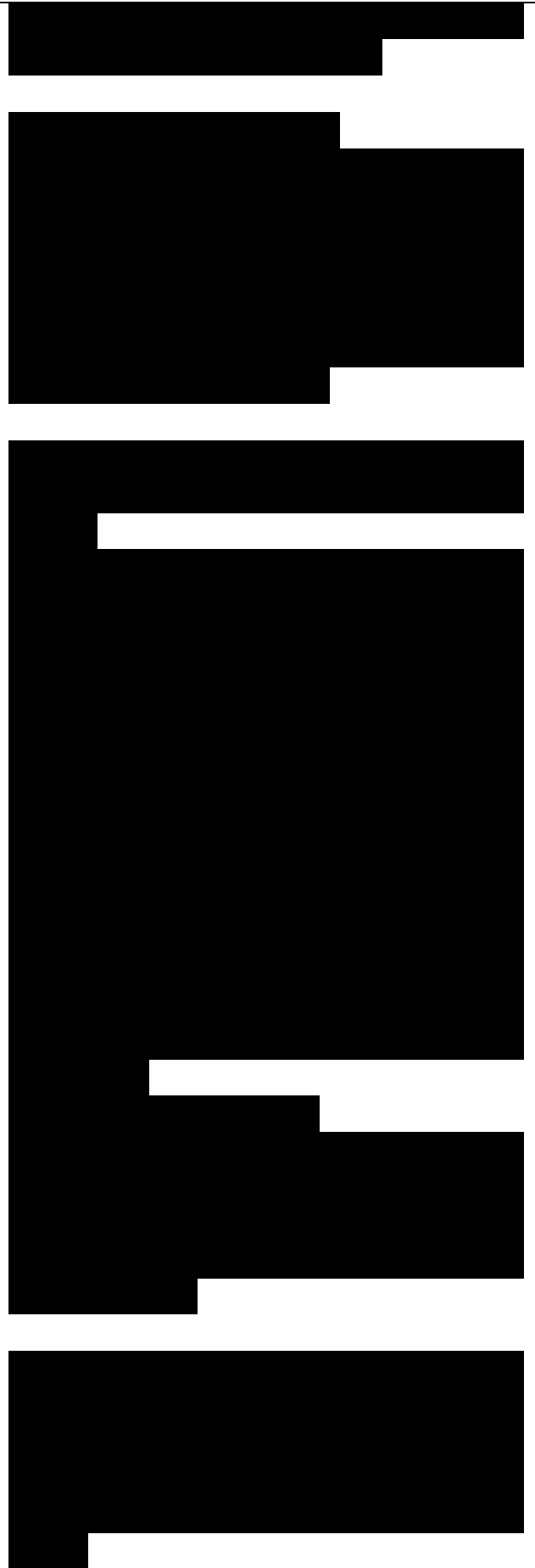
periodic structure, it experiences multiple reflections upon successive periods inside the structure. By adjusting the period and the index of the materials, constructive inter¬ference in reflection can occur such that the light with one wavelength can be reflected completely and the other wavelengths are still transmitted. Light of frequencies lying within the stopband evanesce in this manner.

In a nonlinear periodic device, the spectral position as well as the strength of the stopband may in general be intensity-dependent. The dynamic shift of the stopband can detune a frequency component out from the Bragg condition at high intensities, thus allowing the frequency component to propagate through the system unimpeded - realizing the switching function. Besides switching, periodic nonlinear structures have also been either theoretically predicted or experimentally demonstrated to give rise to pulse compression [6, 7], limiting [8, 9, 10, 11, 12], and logic operations [13, 14]. These potential abilities in self-processing of temporal pulses motivate research into exploring novel designs of nonlinear periodic structures to search for new functionalities and to evaluate their prospective performance.

1.3 Thesis Focus

This thesis considers a specific class of nonlinear periodic structures, investigates and evaluates their potential signal processing abilities, and discusses their practicality. An understanding of the fundamental concepts and previous research are presented in Chap¬ter 2. In order to explore the time-domain signal processing capabilities of the device, theoretical and numerical algorithms are

used to simulate the device performance in the time domain. Chapter 3 describes the analytical framework of the numerical algorithms, and Chapter 4 describes the details of the simulation model for simulating the device performance. Chapter 5 investigates the temporal behavior of the device, demonstrating the limiting and pulse reshaping signal processing abilities.

2.1 Introduction

It was explained in the preceding chapter that nonlinear periodic structures have multiple potential applications in all-optical signal processing. In this chapter, a detailed survey of the literature on the subject of nonlinear Bragg gratings is presented. It begins with a brief summary of some basic concepts of Bragg gratings and nonlinearity and a list of new capacities which can be created by combining the two. Then follows a survey on past research on nonlinear Bragg gratings. The concepts of both solitonic and non-solitonic pulse propagation in these Bragg gratings are discussed. Based on this review, the objective of the thesis is formulated and the remainder of this work is laid out.

The present chapter reviews previous findings on nonlinear Bragg gratings. The chapter lays a foundation for the remainder of the thesis by identifying what is known and what is missing in nonlinear periodic device operations. It proposes an avenue in order to fill the gap identified in the published literature.

2.5 Thesis Organization

The organization of the thesis is as follows:
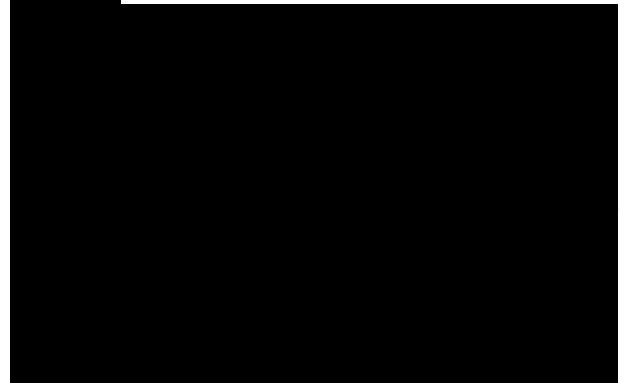
In Chapter 3, the quantitative analytic framework is derived for subsequent deploy¬ment throughout the remainder of this thesis. The coupled-mode equations that describe the evolution of pulse envelopes in a nonlinear Bragg grating are derived. The Bragg soliton solutions of these coupled-mode equations are also obtained mathematically in this chapter. Chapter 4 describes the procedure for a convergent numerical solution of the equations derived. The numerical method for solving the coupled-mode system is explained. The boundary conditions and the balance equations for the system to be satisfied are identified. Also in this chapter, the Bragg structure studied in this thesis is defined and the material parameters chosen for the numerical simulations are stated and justified. Both solitonic (expressions defined in Chapter 3) and non-solitonic pulses are explained. Chapter 5 reports on three sets of time-domain analyses of ultrashort pulse propagation through different Bragg gratings with alternating oppositely-signed Kerr co¬efficients: (i) 0 linear grating; (ii) in-phase linear grating; (iii) out-of-phase linear grating. The term in-phase linear grating refers to as the case when the material with the higher linear index has a positive Kerr coefficient, and the material with the lower linear index has a negative Kerr coefficient. Similarly, the term out-of-phase linear grating means that the material with lower linear index has a positive Kerr coefficient, and the material with higher linear index has a negative Kerr coefficient. The numerical simulation results and the mechanisms behind the observations are discussed. The thesis concludes in

Chapter 6 with an overview of the significant contributions made to optical signal processing and suggests future research directions.

3.1 Introduction

Before exploring the time-domain signal processing capabilities of the device, it is neces¬sary to return to the fundamentals to distill the essential elements of Maxwell's equations which require attention for understanding the evolution of pulses across a nonlinear peri¬odic structure. Different sets of coupled-mode equations which describe the pulse propa¬gation in nonlinear periodic structures have been derived previously for the study of gap solitons. The present chapter derives a set of coupled-mode equations which capture the physical mechanisms of one class of stable nonlinear periodic structures.

3.2 Approximation of the Refractive Index Function

The device under consideration consists of materials of alternating, oppositely-signed Kerr coefficients, as illustrated earlier in Figure 2.3. If the variations of the refractive in¬dex due to the combined effect of linear and nonlinear index differences in the constituent repeated subunits are much smaller than the average index, the index of refraction profile $nA(z, |E|2)$ can be approximately viewed as a periodic function along the spatial prop¬agation direction of the structure, as illustrated in Figure 3.1. The function $nA(z, |E|2)$

Refractive Index $n(z, |E|2)$

Figure 3.1: Refractive index profile of the Bragg grating device along the spatial propa¬gation direction.

may be described analytically over one
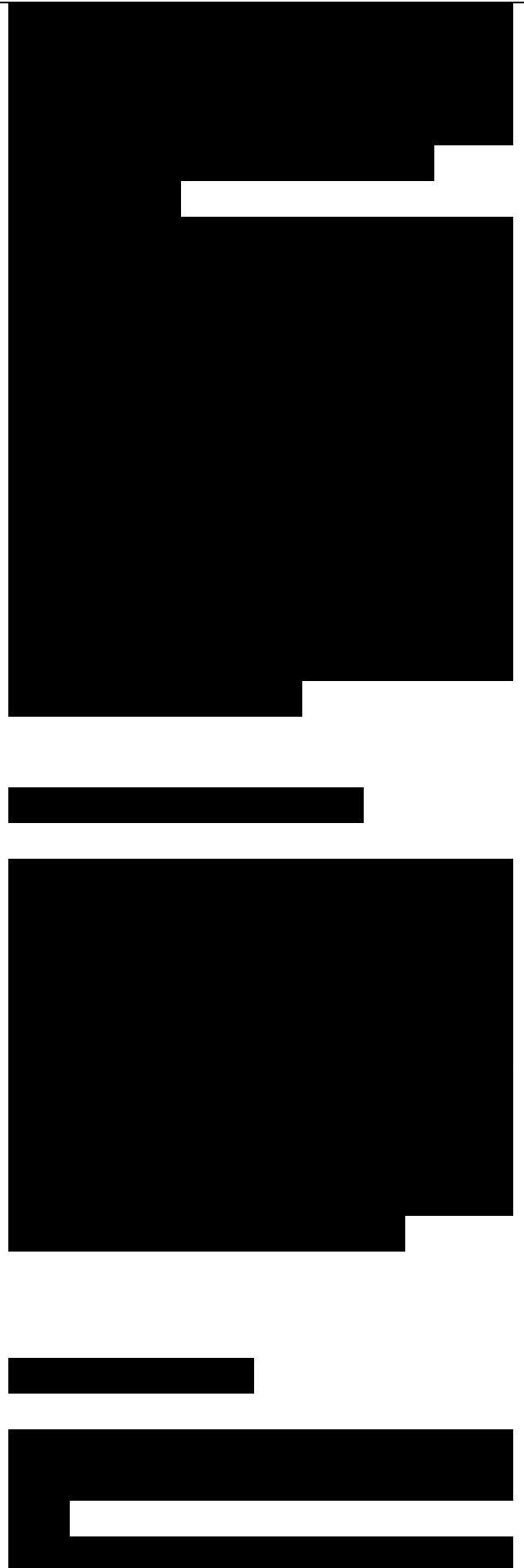
period, as follows:

$n_0^2 + n_{,,i}^2|E|^2$, if $f < z < n^{\wedge}$; $n = 1, 2,...$

with the periodic medium being a N-layered quarter-wave stack. By using a Fourier series expansion of this function, $nA(z, |E|^2)$ in Eq. (3.1) can be resolved into a infinite sum of sine and cosine terms:

where fo is the fundamental frequency: $f_o — 1/A$. The coefficients of an and bn represent the amplitudes of the even and odd terms, respectively. The quantity nfo represents the nth harmonic of the fundamental frequency fo. The coefficient ao is the mean value of the periodic signal $nA(z, |E|^2)$ over one period, as shown by the time average:

Coefficients an and bn are:

For an even function such as the one shown in Figure 3.1, it can be proven that bn = 0 and an = 0. By substituting Eq. (3.1) into Eq. (3.3), we obtain

Similarly, the Fourier coefficient an can be evaluated as:

, if n is even

$n(n_{01} - n_{02} + n_{nl1}|E|^2 - n_{nl2}|E|^2)$ $\sin(n^*)$, if n is odd

Therefore, the index-of-refraction in Eq. (3.2) can be rewritten as: $nA(z, |$

To simplify the above equation, four new parameters are introduced: linear index differ¬ence (nok), average Kerr coefficient (nnl), average linear index (nln), and Kerr coefficient difference (n2k):

Defining the wave number k as $k — $, Eq. (3.7) can be rewritten as:

$nA(z, |E|^2) — n_{ln} + n_{nl}|E|^2 + 2n_{ok}\cos kz + 2n_{2k}|E|^2 \cos kz$ (3.9)

3.3 Derivation of the Coupled-Mode Equations

The electromagnetic wave equation states:

where c — 1/^eo^o is the speed of light and E(z,t) is the electric field.

$E(z,t)$ — $A+(z,t)ei(fc°z-w°4)$ + $A\_(z,t)e-i(fc°z+W0t)$ + higher-order terms. (3.11)

wo — cko/|nln| is the center frequency of a pulse, c is speed of light, and ko — 2n|nln|/Ao is the wave number of the light. A+ and A- are the slowly-varying envelope amplitudes of the incident and reflected waves. Peak reflectance occurs at the center of a forbidden band (Ao) which can be written as Ao — 2nlnA from Eq. (2.1). In other words, resonance in the first bandgap occurs when k = 2k0. Substituting Eq. (3.11) into Eq. (3.10), we obtain the first term as:

and the second term in Eq. (3.10) becomes

(neglected all higher terms in n2k) k0 ^0C

The intensity term |E |2 in the above equation can be expressed in terms of A+ and A_as:

Then Eq. (3.13) can be simplified to:
(3.15)

Thus, Eq. (3.10) can be represented in terms of A+ and A- by combining Eq. (3.12) and (3.15). If we group all the ei(fc°z-wot) terms, we obtain

Using product expansions and simplification, the above equation becomes

Similarly, by grouping all the e i(fc°z+Wot) terms, we obtain the second coupled-mode equation:

To simplify the two coupled-mode equations (Eq. 3.17 and 3.18) further, the spatial coordinate Z and time

parameter T are introduced, where Z —
woz/c and T — wot/nln. This process of
parameter normalization ensures the
spatial and time parameters are of the
same unit; hence making the numerical
analysis easier. The resulting
normalized coupled-mode equations
are:

3.5   Summary

In this chapter, a system of coupled-
mode equations were developed for
wave amplitudes in time and space
based on a Fourier series expansion of
linear and nonlinear refractive indices in
a nonlinear periodic structure. The
coupled-mode equations derived here
are rearranged for the special stable
class of nonlinear periodic structures
consisting of al¬ternating Kerr
nonlinear materials. In the next chapter,
a simulation model built based upon this
system is described.

4.6   Summary

In this chapter, the model of pulse
propagation inside a nonlinear periodic
medium was further elaborated.
Specifically, the range of realistic
physical material parameters was
defined; a numerical algorithm was
described; and the two were combined
to produce preliminary results for
solitonic and non-solitonic pulse
propagation. The analytical model of
Chapter 3, together with the numerical
methods and physical parameters of
Chapter 4, form the basis for the
explorations of nonlinear pulse
propagation presented in Chapter 5.

5.1   Introduction

Optical limiting was predicted from the
steady-state analysis of nonlinear
periodic struc¬tures with oppositely-

signed Kerr coefficients [11]. What would be the temporal response of such device? What applications can such a device be utilized for? This chapter en¬deavors to find answers to these questions - matters of both fundamental and application- oriented interest. It describes the original numerical results obtained from the simulation model in the preceding chapter, revealing the limiting, pulse reshaping, and the S-curve transfer functions. Detailed time-domain analyses of the nonlinear pulse propagation through three different grating strengths are presented. The mechanisms which deter¬mine the behavior of the pulse as it propagates are also identified.

6.1   Thesis Overview

In present-day networks, most of the complex signal-processing operations such as switch¬ing, logic functions, or routing are performed in the electrical domain. This necessi¬tates costly electro-optical (EO) and opto-electrical (OE) conversions. The intent of this work was to investigate the suitability of a nonlinear Bragg structure with alternating oppositely-signed Kerr coefficients for high-speed all-optical time-domain signal process¬ing. Such a device would reduce the need for repeated EO and OE conversions.

Chapter 2 discussed the basic concepts of Bragg gratings and nonlinearity in order to establish a understanding of the topic of nonlinear periodic structures. Previous research on this topic was reviewed. Although many different nonlinear periodic structures have been studied in the past, one important class of stable devices, those with alternating
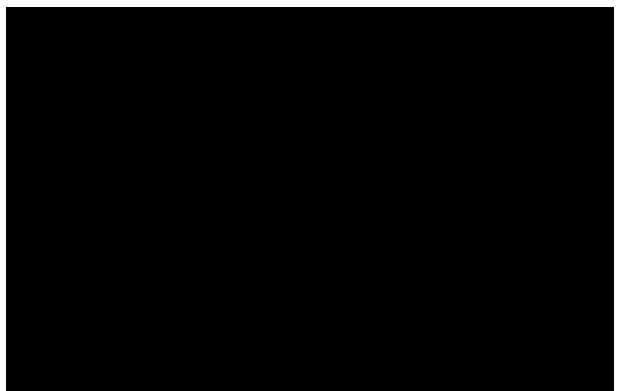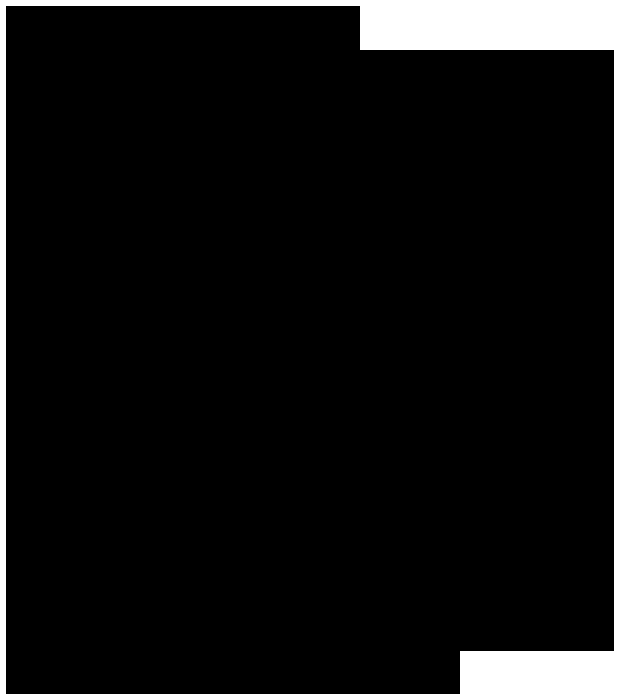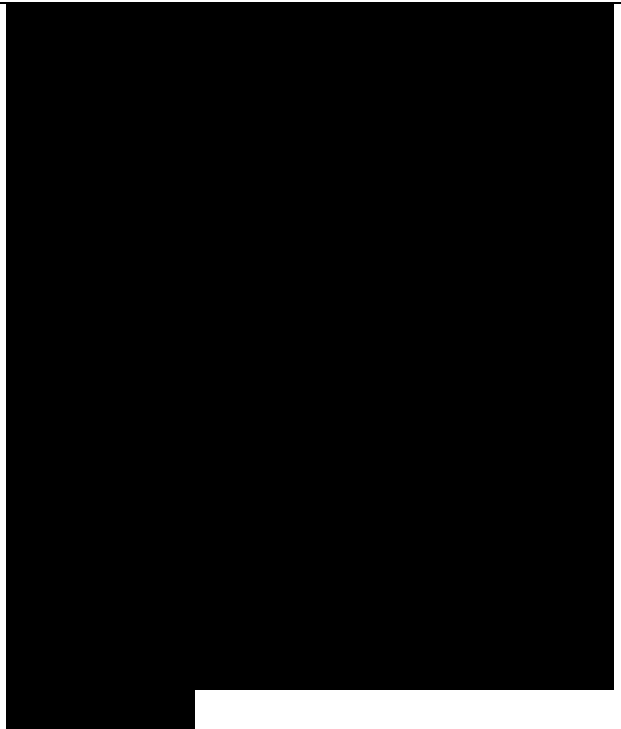
layers of nonlinear materials with balanced Kerr coefficients, had been neglected. It was therefore proposed to study the temporal response of such stable devices.

Chapter 3 derived a system of coupled-mode equations which captures the physical mechanisms of this class of stable nonlinear periodic devices. Under special circum¬stances, a Bragg soliton may propagate. The exact solutions for a Bragg soliton were solved from the coupled-mode system in this chapter.

The analytical framework described in Chapter 3 was necessary in developing a con¬vergent numerical solution of the equations. In Chapter 4, the implementation of this simulation model was presented. The boundary conditions were stated and the device pa¬rameters were defined and justified according to the experimental literature for nonlinear materials properties. Simulations of Bragg soliton and non-solitonic pulse propagation were presented to validate the method of numerical solution.

Chapter 5 presented three sets of numerical analyses of nonlinear pulse propaga¬tion through three different grating strengths: no built-in linear grating, in-phase linear grating, and out-of-phase linear grating. The pulse propagation in each case was de¬scribed and the mechanisms which determine the behavior of the pulses were identified. In the absence of the linear grating, the limiting behavior of the device was concluded to be pulse-bandwidth-dependent. Here, the mechanisms behind pulse shape formation for long-duration pulses were distinguished from those for short-duration pulses. In the presence of the

out-of-phase linear grating, S-curve transfer characteristics were predicted and explored. The simulation results were also used to illustrate and explain the pulse compression effect. A mathematical proof was provided to confirm the understanding of this effect.

6.3   Future Prospects

It is clear that in order to advance networks beyond the rate of electronics, there is a push to do more with optics and less with electronics in the core of the network. This work presented the theoretical analysis of a stable class of one-dimensional nonlinear periodic devices and predicted the design requirements for their time-domain processing functions. However, the model developed for this work does not include linear absorption, nor does it account for saturation of the nonlinearity. Furthermore, the time response of the nonlinear materials with Kerr coefficients on the order of 10_12 cm2/W was assumed to be small relative to the widths of pulses considered. Following are a few future directions for the continuation of this work:

•   Extend the physical model to account for absorption, saturation of the Kerr non¬linearity, and a material response time comparable to the pulse evolution time.

•   Extend the theoretical work to two-dimensional devices to provide confinement in the lateral dimension.

•   Further extend the numerical model to the consideration of three-dimensionally periodic devices. This corresponds to an implementation, currently being devel¬oped at the University of Toronto, of colloidal

crystal-based self-organized photonic crystals whose constituent periodic repeat units consist of Kerr-nonlinear materials with nearly-matched linear refractive indices. The model would result in a series of coupled-mode equations which account for modes strongly coupled via vectors of the reciprocal photonic lattice.